2015 American Control Conference
Palmer House Hilton
July 1-3, 2015. Chicago, IL, USA

Multivariable Predictive Control of Laser-Aided Powder Deposition Processes*

Xiaoqing Cao, Beshah Ayalew

Abstract— **This paper derives and illustrates a multivariable predictive control scheme for laser-aided powder deposition (LAPD) processes utilizing a mobile co-axial laser and powder nozzle. First, a control-oriented multi-input-multi-output (MIMO) process model is adopted that captures the coupled nonlinear dynamics of deposited layer height and average melting pool temperature, with laser power and scanning speed as process inputs. Then, a nonlinear model predictive control (NMPC) scheme is devised in a transformed spatial coordinate system for simultaneous online control of deposition height and melting pool temperature. The conditions that ensure the closed-loop stability of the proposed control scheme are also provided. The effectiveness of the approach as well as the clear trade-offs in the multivariable control is illustrated via a case study on a single layer deposition process.**

Keywords: laser-aided powder deposition, multivariable control, nonlinear MPC

I. INTRODUCTION

Laser-aided powder deposition (LAPD) encompasses a wide range of additive manufacturing (AM) applications such as laser cladding, selective laser sintering (SLS), laser metal deposition (LMD), laser solid freeform fabrication (LSFF), etc. Most LAPD systems consist of laser energy delivery system, powder feeder system and motion system like robotic manipulators or CNC tables [1]. These correspond to the most important manipulated variables in LAPD processes, namely laser power, powder feedrate and scanning speed. Furthermore, due to possible fluctuations in process parameters as well as environmental disturbances, actual process outputs may deviate significantly from the desired values. Thus, closed-loop monitoring and control are needed in order to achieve satisfactory product quality in terms of surface roughness, dimensional accuracy and residual stresses [1]. Often the primary objective is to deposit a layer with a desired height, either of a uniform layer thickness as in laser cladding or of variable thickness in LSFF with complex part geometry. Moreover, the temperature of the melting pool is shown to affect the dilution/penetration depth, thermal distortion/residual stresses and even the dimension of deposited components [1, 2]. Therefore, both the deposited layer height and melting pool temperature need to be controlled simultaneously during LAPD processes.

In the literature, the most commonly proposed control system designs for such processes are proportional-integral-derivative (PID) controllers and their extensions [3, 4]. Recently, advanced control strategies such as the variable structure control [5] and iterative learning control [6] have been proposed for closed-loop regulation of related processes. However, these proposed control schemes were only shown to regulate a specific process output by adjusting a corresponding input in single-input-single-output (SISO) manner. In [7], a two-input-single-output (MISO, two inputs to the *controller*) hybrid control system that includes a master height controller and a slave temperature controller is designed to control both layer height and melting pool temperature in a direct metal deposition process. Although this expands the potential of controlling multiple *process* outputs simultaneously, a control system design via a single control variable, such as the laser power, has limited capabilities as pointed out in [2, 7]. This recognition motivates the inclusion of another control variable, such as the laser scanning speed, to achieve effective process control in a wider range of operating conditions [2].

To design a suitable MIMO control system for LAPD processes, the following issues need to be considered: 1) given the nonlinear coupling between layer height and melting pool temperature, simultaneous regulation of these two variables is highly desirable; 2) there are practical constraints on the individual control input variables or process states, such as the maximum laser power, scanning speed or allowable pool temperature. Model predictive control (MPC), also referred as receding horizon control (RHC), is well-suited to address both issues in LAPD processes given its well-known ability to deal with hard constraints in the control of multivariable plants [8]. The main idea of MPC is to use an explicit plant model to predict system behavior in a prediction horizon. Therein, an optimal open-loop input sequence is computed to satisfy desired optimization criteria and constraints of the process. Only the first input in this optimal sequence is often applied to the actual plant. Input constraints and some state constraints may be formulated explicitly as inequality conditions while the process control objectives can be enforced by properly designed cost functions in the MPC formulation.

Like any other control system, stability is one of the most important issues with MPC. As pointed out in [9], closed-loop stability cannot be guaranteed with the general MPC formulation because of the finite-horizon open-loop optimization inherent in it. Although it may be possible to stabilize the control system by tuning the design parameters such as horizon length or weighting matrices in the objective functions [10], more systematic methods are often needed for general applications. Early works in this area include the infinite-horizon formulation [11] and the finite-horizon formulation with terminal state equality constraints [12] to ensure closed-loop stability. However, these methods are

*Research supported, in part, by US National Science Foundation under Grant No. CMMI-1055254, and the U.S. Department of Energy (DOE) GATE program under Grant No. DE-EE0005571.

Xiaoqing Cao and Beshah Ayalew are with the Applied Dynamics and Control Group at the Clemson University-International Center for Automotive Research, Greenville, SC 29607 USA (e-mail: {xiaoqin, beshah@clemson.edu}).

either impractical or computationally intractable due to the hard terminal equality constraints. By adding a terminal state penalty in the objective function and defining a terminal state constraint region (terminal state inequality), it is shown that the stability conditions can be relaxed and closed-loop stability can still be achieved via a local stabilizing controller inside the terminal region [13, 14].

In this paper, we first describe a control-oriented MIMO process model that captures the coupled nonlinear dynamics of deposited layer height and melting pool temperature for LAPD processes utilizing a mobile co-axial laser and powder nozzle. A coordinate transformation is introduced to conveniently express the MIMO process model in the spatial domain for the subsequent nonlinear model predictive controller (NMPC) design. Herein lies the main contribution of the paper: it devises a MIMO NMPC scheme for simultaneous online regulation and tracking of two process outputs (deposited layer height and melting pool temperature) by manipulating at least two input variables (laser power and scanning speed). The conditions for closed-loop stability of the NMPC approach to the MIMO control of LAPD processes are also derived and made explicit.

The rest of the paper is organized as follows: Section II presents the LAPD process model. Section III details the formulation of the NMPC scheme and the corresponding sufficient conditions for closed-loop stability. Section IV provides case studies where the effectiveness of the proposed multivariable control scheme is demonstrated. Conclusions are included in Section V.

II. Models of LAPD Processes

A. Process Overview

The essence of LAPD processes can be illustrated in Fig. 1. A laser beam with high power intensity sweeps on the surface of the substrate, creating a melting pool. The powder material is either pre-placed on the substrate or injected into the melting pool by coaxial or lateral powder nozzles. After the melting and solidification processes, a metallurgical bond is formed between the deposited layer and the substrate. Products with complex geometries can be manufactured in a layer by layer manner.

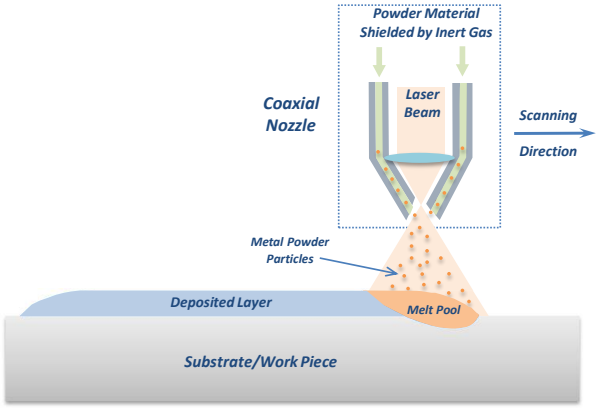

Fig. 1. Schematic of the LAPD processes

B. Control-Oriented MIMO Process Model

In this section, the control-oriented model for LAPD process is briefly discussed. This model is first proposed in our companion modeling work for LAPD processes [15]. The main characteristic of this model is that it captures the coupled dynamics of deposited layer height and average melting pool temperature while limiting the model complexity to a nonlinear state-space form. The schematic of the proposed model is illustrated in the following figure:

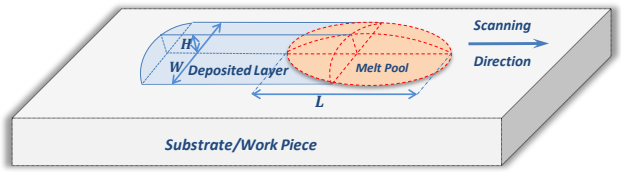

Fig. 2. Schematic of the control-oriented process model

The above figure describes the geometry of the melting pool, which is approximated by a semi-ellipsoid with length L, width W and height H [4]. Additionally, the aspect ratio (width/length) of the melting pool is assumed to be empirically related to laser power and scanning speed by [16]:

$$\frac{L}{W} = 1 + (Dq + E)v \tag{1}$$

where D and E are positive constants. Furthermore, considering that the deposited track-width remains approximately the same during the process and is determined by laser beam diameter [17], a constant track width denoted by W_0 is assumed in this model.

Similar to the SISO semi-empirical model proposed in [3], the derivation of this control-oriented MIMO model is a concatenation of the steady-state input-output relations and a first-order process dynamics. The structure of this Hammerstein type model is shown in Fig. 3.

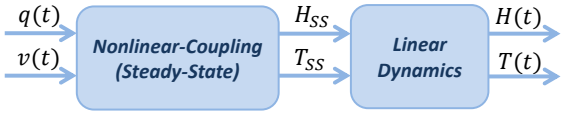

Fig. 3. Structure of the control-oriented process model

where H_{ss} and T_{ss} denote the nonlinear relationships between steady-state layer height and melting pool temperature. These coupled steady-state relations are derived from conservation laws of mass and energy in the melting pool [4]. The mass balance can be expressed as:

$$\rho \dot{V} = \eta_m \dot{m}_P - \rho A v \tag{2}$$

where $V = \frac{\pi}{6} W_0 H L$ is the total volume of the melting pool; $A = \frac{\pi}{4} W_0 H$ is the crosssection area in the transverse plane; $\eta_m \dot{m}_P$ denotes the amount of powder material that is deposited into the melting pool in unit time and η_m is the powder catch efficiency (ratio of deposited powder with respect to total injected powder). Given the fact that: 1) powder material is only deposited into the melting pool area (where $T > T_m$, T_m is the melting temperature); 2) the maximum powder catch efficiency is mainly determined by the nozzle configuration (standoff distance, laser beam

distribution, powder distribution, etc.), the powder catch efficiency can be further modeled by a temperature-dependent function as:

$$\eta_m(T) = \begin{cases} \eta_{m0} * \left[1 - e^{-k_T(T-T_m)}\right], T > T_m \\ 0, T \le T_m \end{cases} \quad (3)$$

where $\eta_{m0} \in [0,1]$ is the maximum powder catch efficiency and is assumed to be a positive constant, defined by the selected nozzle configuration. With constant laser power and scanning speed, the melting pool geometry remains approximately the same in a coordinate system that moves with the laser source. Thus, the steady-state (in the moving coordinate) deposited layer height can be obtained by setting the left term in the mass balance equation (2) equal to zero:

$$H_{ss} = \frac{4\eta_m \dot{m}_P}{\pi \rho W_0 v} \quad (4)$$

Similarly, the energy balance in the melting pool is:

$$\rho(\dot{V\epsilon}) = \eta_q q - A_s h_s (T - T_m) - A_g h_g (T - T_0) - \delta_{S/L} \quad (5)$$

This expresses the fact that the variation of total energy in the melting pool is equal to the difference between absorbed laser energy and heat transfer due to convection and melting/solidification in the melting pool. The specific internal energy ϵ is defined as: $\epsilon(T) = C_s(T_m - T_0) + \mathcal{L} + C_l(T - T_m)$, where C_s/C_l and h_s/h_g denote the solid/liquid heat capacity and solid/gas heat convection coefficient, respectively. The heat convection area on these two interfaces can be expressed by: $A_s = \frac{\pi}{4} W_0 L$, $A_G = 2\pi * \left(\frac{\left(\frac{W_0}{2} * \frac{L}{2}\right)^{1.6} + \left(\frac{W_0}{2} * H\right)^{1.6} + \left(\frac{L}{2} * H\right)^{1.6}}{3} \right)^{1/1.6}$. $\mathcal{L}$ is the latent heat of fusion during the melting process. During laser irradiation, both the laser power and scanning speed affect the melting pool surface geometry, which further determines the area of laser beam absorption. Therefore, the laser absorptivity can be modeled as a function of laser power and scanning speed as follows:

$$\eta_q(q, v) = \eta_{q0} * (1 - e^{-k_q q}) * e^{-k_v v} \quad (6)$$

where η_{q0}, k_q, k_v are positive constants. The last term $\delta_{S/L}$ in the energy balance equation represents the power outflow from the melting pool due to the effect of solidification and melting. In steady state, the melting pool moves at the same speed as the laser source and the pool geometry remains approximately the same. Therefore, the solidification and melting speed can be assumed the same and the term $\delta_{S/L}$ vanishes. The steady-state temperature can be obtained as:

$$T_{ss} = \frac{\eta_q q + A_s h_s T_m + A_g h_g T_0}{A_s h_s + A_g h_g} \quad (7)$$

As pointed out in [3], the dynamics of LAPD processes are dominated by thermal effects which can be approximated with a linear first-order dynamics. With this, the final equations of the Hammerstein model (Fig. 3) are [15]:

$$SYS_t: \begin{cases} \dot{H} = \frac{1}{\tau_H} * \left(\frac{4\eta_m \dot{m}_P}{\pi \rho W_0 v} - H \right) \\ \dot{T} = \frac{1}{\tau_T} * \left(\frac{\eta_q q + A_s h_s T_m + A_g h_g T_0}{A_s h_s + A_g h_g} - T \right) \end{cases} \quad (8)$$

where τ_H and τ_T are time constants.

In this MIMO model, laser power and scanning speed are selected to be the control input variables. The typical response of powder delivery system is so slow that it can be considered pre-set [2]. Both process outputs, which are deposited layer height and melting pool temperature, are assumed to be measureable. This can be achieved via appropriate sensors such as high-speed CCD cameras for deposited layer height sensing and radiation pyrometers for melting pool temperature measurement [7]. Moreover, process configuration parameters such as the nozzle standoff distance/orientation, laser beam radius, powder feedrate and distribution, are assumed to be fixed. This assumption arises from the persistent trade-off between model fidelity and computational efficiency in control system design.

Remark 1: It is worth to point out that the dynamic MIMO model adopted in this paper is derived from quasi-steady state relations with the laser source *moving* at constant speed. Thus, it only addresses the *in-process* dynamics of the LAPD process with moving laser source. Correspondingly, the multivariable predictive control proposed below is also aimed for in-process control. The physical phenomena involved for the beginning and end of the process, where the melting pool develops and disappears, are far more complex and thus require more detailed modeling techniques. The control design for the specific beginning and end phase of the process is beyond the scope of this paper. For more details on this topic, readers are referred to [18]. However, in the above model, special attention should be paid to the singularity $v = 0$ by providing a minimum operating speed constraint.

In this paper, we mainly focus on using the model for the multivariable control system design in LAPD processes. The calibration of the parameters in the above model is detailed in our companion paper [15] and is listed briefly in Table I.

TABLE I. IDENTIFIED PARAMETERS IN PROPOSED MODEL

Variable	Value	Variable	Value
τ_H	0.1145 $[s]$	η_{q0}	0.0545 [1]
τ_T	0.2898 $[s]$	k_q	$1.357 * 10^{-4}$ $[1/W]$
η_{m0}	0.4224 [1]	k_v	332.8 $[s/m]$
k_T	0.0072 [1/K]	D	-0.0769 $[s/m/W]$
		E	-0.9071 $[s/m]$

III. MULTIVARIABLE PREDICTIVE CONTROL

In this section, the specific control problem is first formulated based on the above MIMO process model. This is then followed by the derivation of closed-loop stability conditions for the proposed predictive control scheme.

A. Control Problem Formulation

The control problem can be defined as regulating or tracking the deposited layer height H and melting pool temperature T towards their desired values H_d and T_d, by adjusting the control inputs: laser power q and scanning speed

v. In LAPD processes, the spatial domain (the deposition track length) is often fixed, the desired part geometry is predefined, and the deposition route is pre-planned. Since the scanning speed is a manipulated control input, the process time domain is not necessarily fixed (e.g. leading to a variable prediction horizon in time for MPC). Thus, to facilitate the predictive controller design, a coordinate transformation is first introduced to express the process model in a spatial S-coordinate of the same direction as that of the laser motion:

$$\begin{cases} \dot{H} = \dfrac{dH}{ds}\dfrac{ds}{dt} = \dfrac{dH}{ds}v \\ \dot{T} = \dfrac{dT}{ds}\dfrac{ds}{dt} = \dfrac{dT}{ds}v \end{cases} \tag{9}$$

where s denotes the variable in the spatial S-coordinate and ds is defined as the infinitesimal in this coordinate analogous to dt in the time domain. The MIMO process model in S-coordinate can then be written as:

$$SYS_S: \begin{cases} \dfrac{dH}{ds} = \dfrac{1}{v} * \dfrac{1}{\tau_H} * \left(\dfrac{4\eta_m \dot{m}_P}{\pi\rho W_0 v} - H\right) \\ \dfrac{dT}{ds} = \dfrac{1}{v} * \dfrac{1}{\tau_T} * \left(\dfrac{\eta_q q + A_s h_s T_m + A_g h_g T_0}{A_s h_s + A_g h_g} - T\right) \end{cases} \tag{10}$$

Assume that the coordinate-dependent desired layer height and melting pool temperature are H_d and T_d, respectively. Define the tracking errors as:

$$e_H = \frac{H - H_d}{H_0}; e_T = \frac{T - T_d}{T_m} \tag{11}$$

where H_0 is the nominal layer height. The dynamical model of the tracking error can be expressed as:

$$SYS: e' = \begin{bmatrix} e_H' \\ e_T' \end{bmatrix} = \begin{bmatrix} F_1(e_H, e_T; u_2) \\ F_2(e_H, e_T; u_1, u_2) \end{bmatrix} = F(e, U) \tag{12}$$

where $e = \begin{bmatrix} e_H \\ e_T \end{bmatrix}$ and the superscript $(')$ denotes the first-order derivative in S-coordinate; $U = \begin{bmatrix} u_1 \\ u_2 \end{bmatrix} = \begin{bmatrix} q/\bar{q} \\ v/\bar{v} \end{bmatrix}$ is the control input vector, which contains the laser power and scanning speed. $\bar{q}$ and $\bar{v}$ denote the upper bounds of control input variables, respectively. The nonlinear functions F_1 and F_2 are short for:

$$F_1 = \frac{1}{H_0}\left[\frac{1}{u_2 \bar{v} \tau_H}\left(\frac{4\eta_m \dot{m}_P}{\pi\rho W_0 \bar{v} u_2} - H_0 e_H - H_d\right) - H_d'\right] \tag{13}$$

$$F_2 = \frac{1}{T_m}\left[\frac{1}{u_2 \bar{v} \tau_T}\left(\frac{\eta_q u_1 \bar{q} + A_s h_s T_m + A_g h_g T_0}{A_s h_s + A_g h_g} - e_T T_m - T_d\right) - T_d'\right] \tag{14}$$

The control objective is to find a suitable control input vector $U(s)$ which drives the tracking error to zero. We seek to achieve this with a nonlinear MPC framework. The objective function $J(s_0, e, U)$ is defined as follows:

$$J = \int_{s_0}^{s_0 + s_p} \mathbb{C}\left(e(\varsigma), U(\varsigma)\right) d\varsigma + P\left(e\left(s_0 + s_p\right)\right) \tag{15}$$

where s_0 denotes the current laser position and s_p is the predictive horizon in the spatial S-coordinate. The first function is defined as: $\mathbb{C}\left(e(\varsigma), U(\varsigma)\right) = e(\varsigma)^T Q e(\varsigma) + U(\varsigma)^T R U(\varsigma)$, where $Q = \begin{bmatrix} q_{11} & 0 \\ 0 & q_{22} \end{bmatrix}, R = \begin{bmatrix} r_{11} & 0 \\ 0 & r_{22} \end{bmatrix}$ are positive definite matrices with $q_{11}, q_{22}, r_{11}, r_{22} > 0$. The terminal state penalty in the objective function is defined as:

$$P\left(e\left(s_0 + s_p\right)\right) = \frac{1}{2} e\left(s_0 + s_p\right)^T e\left(s_0 + s_p\right) \tag{16}$$

The optimization problem (OP) for the MPC is formulated as:

$$min_U J(s_0, e, U) \tag{17}$$
$$Subject\ to: \begin{cases} e'(\varsigma) = F\left(e(\varsigma), U(\varsigma)\right) \\ U(\varsigma) \in \mho \\ e\left(s_0 + s_p\right) \in \Omega \end{cases}$$

where $\mho$ denotes the admissible input set and Ω is the terminal state constraint region, which is imposed for closed-loop stability and $\varsigma \in \left[s_0, s_0 + s_p\right]$.

B. Closed-Loop Stability Conditions

In this paper, the closed-loop stability of LAPD processes with the proposed nonlinear MPC scheme is analyzed based on the following theorem re-stated from [13, 14].

Theorem 1 [13, 14]: Suppose the reference control signals are bounded and the OP is feasible at $\varsigma = s_0$. The model predictive control algorithm described previously for the system (SYS) is asymptotically stable if a terminal state controller $U_T\left(s_0 + s_p\right)$ exists such that the following condition is satisfied:

$$P'\left(e\left(s_0 + s_p\right)\right) + \mathbb{C}\left(e\left(s_0 + s_p\right), U\left(s_0 + s_p\right)\right) \leq 0 \tag{18}$$

for any state $e\left(s_0 + s_p\right)$ belonging to the terminal region Ω.

In the following, we analyze the terminal state in LAPD process. The coordinate variable $s_0 + s_p$ is omitted for brevity. According to Theorem 1, we have:

$$\begin{aligned} &P'(e) + \mathbb{C}(e, U) = e^T e' + e^T Q e + U^T R U \\ &= \begin{bmatrix} e_H & e_T \end{bmatrix} \begin{bmatrix} F_1 \\ F_2 \end{bmatrix} + q_{11} {e_H}^2 + q_{22} {e_T}^2 + r_{11} {u_1}^2 + r_{22} {u_2}^2 \\ &= \frac{1}{H_0 \bar{v} \tau_H} * \frac{4\eta_m \dot{m}_P}{\pi\rho W_0 \bar{v}} * \frac{e_H}{{u_2}^2} - \frac{1}{\tau_H \bar{v} u_2} * {e_H}^2 - \frac{1}{\tau_T \bar{v} u_2} * {e_T}^2 \\ &\quad - \left(\frac{H_d}{H_0 \tau_H \bar{v} u_2} + \frac{H_d'}{H_0}\right) * e_H - \left(\frac{T_d}{\tau_T T_m \bar{v} u_2} + \frac{T_d'}{T_m}\right) * e_T \\ &\quad + \frac{1}{\tau_T T_m \bar{v}} * \frac{\eta_q u_1 \bar{q} + A_s h_s T_m + A_g h_g T_0}{A_s h_s + A_g h_g} * \frac{e_T}{u_2} + q_{11} {e_H}^2 \\ &\quad + q_{22} {e_T}^2 + r_{11} {u_1}^2 + r_{22} {u_2}^2 \end{aligned} \tag{19}$$

Define the terminal control as:

$$U_T = \begin{bmatrix} u_1 \\ u_2 \end{bmatrix} = \begin{bmatrix} -K_1 u_2 e_T \\ K_2 \end{bmatrix} \tag{20}$$

where K_1, K_2 are positive constants. Then, equation (19) can be rewritten as:

$$\begin{aligned} &P'(e) + \mathbb{C}(e, U) \\ &= \left(\frac{1}{H_0 \bar{v} \tau_H} * \frac{4\eta_m \dot{m}_P}{\pi\rho W_0 \bar{v} {K_2}^2} - \frac{H_d}{H_0 \tau_H \bar{v} K_2} - \frac{H_d'}{H_0}\right) * e_H \end{aligned}$$

$$+\left(\frac{1}{\tau_T T_m \bar{v} K_2} * \frac{A_s h_s T_m + A_g h_g T_0}{A_s h_s + A_g h_g} - \frac{T_d}{\tau_T T_m \bar{v} K_2} - \frac{T_d'}{T_m}\right) * e_T$$
$$+\left(q_{22} - \frac{1}{\tau_T \bar{v} K_2} - \frac{1}{\tau_T T_m \bar{v}} \frac{\eta_q K_1 \bar{q}}{A_s h_s + A_g h_g} + r_{11} {K_1}^2 {K_2}^2\right) * {e_T}^2$$
$$+\left(q_{11} - \frac{1}{\tau_H \bar{v} K_2}\right) * {e_H}^2 + r_{22} {K_2}^2 \quad (21)$$

According to Theorem 1, the following design parameter constraints and terminal state constraint have to be satisfied:

1) Requirements of parameters:

$$\begin{cases} q_{11} - \frac{1}{\tau_H \bar{v} K_2} \le 0 \\ q_{22} - \frac{1}{\tau_T \bar{v} K_2} + r_{11} {K_1}^2 {K_2}^2 \le 0 \end{cases} \quad (22)$$

2) Terminal state inequality constraint:

$$\left(\frac{1}{\tau_T T_m \bar{v} K_2} * \frac{A_s h_s T_m + A_g h_g T_0}{A_s h_s + A_g h_g} - \frac{T_d}{\tau_T T_m \bar{v} K_2} - \frac{T_d'}{T_m}\right) * e_T$$
$$+\left(\frac{4\eta_m \dot{m}_P}{H_0 \tau_H \pi \rho W_0 \bar{v}^2 {K_2}^2} - \frac{H_d}{H_0 \tau_H \bar{v} K_2} - \frac{H_d'}{H_0}\right) * e_H + r_{22} {K_2}^2 \le 0 \quad (23)$$

Note that by imposing the second inequality in the parameter requirements, the following inequality is implied:

$$q_{22} - \frac{1}{\tau_T \bar{v} K_2} - \frac{1}{\tau_T T_m \bar{v}} \frac{\eta_q K_1 \bar{q}}{A_s h_s + A_g h_g} + r_{11} {K_1}^2 {K_2}^2 \le 0 \quad (24)$$

The design parameters in the terminal control (20) and the objective function (15) should be selected to fulfill the parameter requirements (22). Then, by adding the terminal state inequality (23) into the MPC constraints, the inequality condition (18) is satisfied in Theorem 1.

IV. Case Study

To illustrate the proposed multivariable predictive control scheme, a single layer deposition process (e.g. laser cladding) is considered here as an example of LAPD processes. In this process, a thin coating (cladding layer) is deposited on the top surface of a low-carbon steel substrate with a length of 50 mm. An Nd:YAG laser (wavelength of 1.06 μm) with the maximum power of 1.4 kW is used as the heat source and is assumed delivered from the coaxial nozzle head. The powder particles are selected to be Inconel 718 with an average radius of 50 μm in spherical shape. The scanning speed of the nozzle head is mainly determined by the motion control system and is limited up to 10 mm/s in this application setup. The desired deposition height profile is assumed to be sinusoidal. This is often met in manufacturing complex parts where deposition of a continuously variable geometry is required. Meanwhile, the desired temperature profile has constant levels at different sections (with proper ramp rates) to meet specific thermo-mechanical properties along the track [19].

Two scenarios are considered in control simulations: 1) MISO control with scanning speed as the only process input (controller output, with nominal laser power 600 W); 2) MIMO control with both laser power and scanning speed as the process inputs. The first scenario serves as an example of typical control schemes with single control variable while the second one is used to demonstrate the efficacy of the proposed multivariable control. The design parameters used in the objective function are: $Q = \begin{bmatrix} 1440 & 0 \\ 0 & 510 \end{bmatrix}, R = \begin{bmatrix} 0.0013 & 0 \\ 0 & 0.0013 \end{bmatrix}$ while the parameters in the terminal control are selected to be: $K_1 = 0.05, K_2 = 0.6$. These parameters are selected such that the parameter requirements are fulfilled with $q_{11} - \frac{1}{\tau_H \bar{v} K_2} = -15.6 < 0$ and $q_{22} - \frac{1}{\tau_T \bar{v} K_2} + r_{11} {K_1}^2 {K_2}^2 = -65.1 < 0$. These parameters remain the same in both case studies. The spatial sampling interval is set to be 0.25 mm while the length of both the control and predictive horizon is 2 mm. The parameters used in the simulation are listed in Table II.

TABLE II. Parameters Used in Simulation

Variable	Value	Variable	Value
T_m/T_0	$1809/293[K]$	$\mathcal{L}$	$2.7 * 10^5[J/kg]$
W_0	$2\ [mm]$	$\dot{m}_p$	$8[g/min]$
ρ_l	$7800\ [kg/m^3]$	H_0	$1[mm]$
C_l/C_s	$804/658\ [J/kg/K]$	$\underline{q}/\overline{q}$	$400/1400[W]$
h_s/h_g	$1400/24[W/m^2/K]$	$\underline{v}/\overline{v}$	$2/10[mm/s]$

Simulation results and the comparison between the two control scenarios are illustrated in Figs. 4-6.

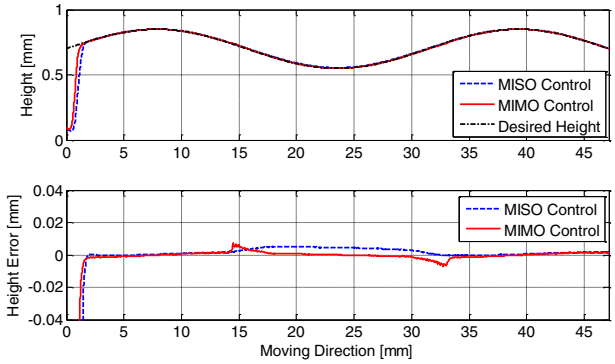

Fig. 4. Deposited layer height under control

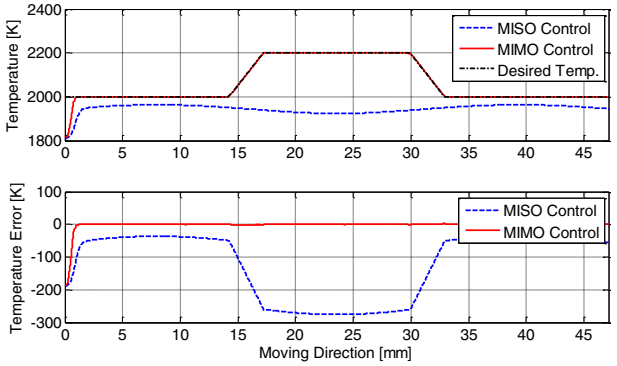

Fig. 5. Melting pool temperature under control

As we can see from Fig. 4, with the selected design parameters, the actual deposited layer is able to follow the desired layer shape under both MISO and MIMO control. The maximum height errors are around 0.004 mm in both cases, which are relatively small compared with the desired layer height. However, the melting pool temperature control

performances demonstrated in Fig. 5 show that with the MISO control where scanning speed is the only control input, the average melting pool temperature fails to follow the desired value along the deposition track. This can be further observed from the large temperature error under the MISO control. This is mainly due to the fact that LAPD is actually a MIMO system with strongly nonlinear coupling between process variables. By adjusting the scanning speed, melting pool temperature can be affected either directly (through temperature dynamics) or indirectly (through height dynamics, which is coupled with temperature dynamics), this effects limit the control performance by adjusting scanning speed alone in the MISO control scheme. By comparison, the proposed multivariable control is able to regulate the temperature towards the desired value while maintaining the prescribed deposited layer shape at the same time. The corresponding control inputs are provided in Fig. 6.

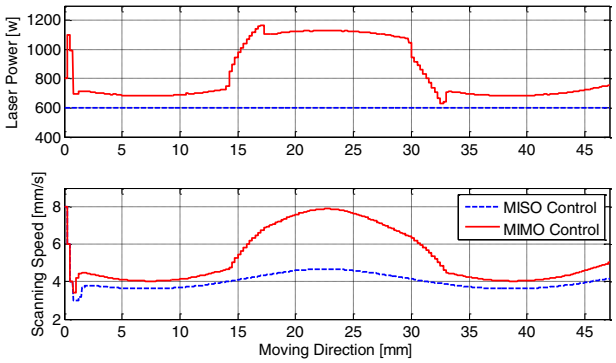

Fig. 6. Control inputs

It is observed that at the beginning of the process, scanning speed is lowered in both cases to increase the deposited layer height. With the proposed MIMO control, scanning speed is higher than that with the MISO control along the whole deposited track, which can be desirable for productivity. However, this is accompanied by the use of higher laser power to compensate for the effect of shorter laser irradiation duration. In fact, this trade-off is tunable with the selections of weighting parameters in the objective function.

V. CONCLUSIONS

In this paper, a multivariable predictive control scheme is proposed for a class of LAPD processes. The inherent MIMO characteristic of these processes is first captured by a control-oriented process model. Then, NMPC is devised to regulate the deposited layer height and melting pool temperature by adjusting laser power and scanning speed simultaneously. A set of stability conditions, which include parameter constraints and the terminal state inequality constraints, are derived to ensure closed-loop stability under the proposed control. Simulation results with the application to laser cladding process illustrated the effectiveness of the proposed control scheme. Finally, we remark that only the nominal stability is addressed with the proposed control scheme in this paper. For practical considerations, robustness analyses combined with the proposed NMPC scheme are needed to accommodate model/plant mismatch or parameter uncertainty. This is part of our future work.

REFERENCES

[1] M. R. Boddu, R. G. Landers, and F. W. Liou, "Control of laser cladding for rapid prototyping—A review," in *Solid freeform fabrication symposium Proceedings*, 2001, pp. 6-8.

[2] D. Salehi and M. Brandt, "Melt pool temperature control using LabVIEW in Nd: YAG laser blown powder cladding process," *The international journal of advanced manufacturing technology,* vol. 29, pp. 273-278, 2006.

[3] A. Fathi, A. Khajepour, E. Toyserkani, and M. Durali, "Clad height control in laser solid freeform fabrication using a feedforward PID controller," *The International Journal of Advanced Manufacturing Technology,* vol. 35, pp. 280-292, 2007.

[4] C. Doumanidis and Y.-M. Kwak, "Geometry modeling and control by infrared and laser sensing in thermal manufacturing with material deposition," *Journal of manufacturing science and engineering,* vol. 123, pp. 45-52, 2001.

[5] A. Fathi, A. Khajepour, M. Durali, and E. Toyserkani, "Geometry control of the deposited layer in a nonplanar laser cladding process using a variable structure controller," *Journal of Manufacturing Science and Engineering,* vol. 130, p. 031003, 2008.

[6] L. Tang and R. G. Landers, "Layer-to-layer height control for laser metal deposition process," *Journal of Manufacturing Science and Engineering,* vol. 133, p. 021009, 2011.

[7] L. Song, V. Bagavath-Singh, B. Dutta, and J. Mazumder, "Control of melt pool temperature and deposition height during direct metal deposition process," *The International Journal of Advanced Manufacturing Technology,* vol. 58, pp. 247-256, 2012.

[8] D. Q. Mayne, J. B. Rawlings, C. V. Rao, and P. O. Scokaert, "Constrained model predictive control: Stability and optimality," *Automatica,* vol. 36, pp. 789-814, 2000.

[9] H. Chen and F. Allgöwer, "A quasi-infinite horizon nonlinear model predictive control scheme with guaranteed stability," *Automatica,* vol. 34, pp. 1205-1217, 1998.

[10] F. A. Fontes, "A general framework to design stabilizing nonlinear model predictive controllers," *Systems & Control Letters,* vol. 42, pp. 127-143, 2001.

[11] S. a. Keerthi and E. G. Gilbert, "Optimal infinite-horizon feedback laws for a general class of constrained discrete-time systems: Stability and moving-horizon approximations," *Journal of optimization theory and applications,* vol. 57, pp. 265-293, 1988.

[12] D. Q. Mayne and H. Michalska, "Receding horizon control of nonlinear systems," *Automatic Control, IEEE Transactions on,* vol. 35, pp. 814-824, 1990.

[13] W.-H. Chen, D. J. Ballance, and J. O'Reilly, "Model predictive control of nonlinear systems: computational burden and stability," in *Control Theory and Applications, IEE Proceedings-*, 2000, pp. 387-394.

[14] D. Gu and H. Hu, "Receding horizon tracking control of wheeled mobile robots," *Control Systems Technology, IEEE Transactions on,* vol. 14, pp. 743-749, 2006.

[15] X. Cao and B. Ayalew, "Control-Oriented MIMO Modeling of Laser-Aided Powder Deposition Processes," in *2015 American Control Conference (ACC)*, Chicago, IL, 2015.

[16] A. J. Pinkerton and L. Li, "Modelling the geometry of a moving laser melt pool and deposition track via energy and mass balances," *Journal of Physics D: Applied Physics,* vol. 37, p. 1885, 2004.

[17] A. Fathi, E. Toyserkani, A. Khajepour, and M. Durali, "Prediction of melt pool depth and dilution in laser powder deposition," *Journal of Physics D: Applied Physics,* vol. 39, p. 2613, 2006.

[18] D. Hu and R. Kovacevic, "Sensing, modeling and control for laser-based additive manufacturing," *International Journal of Machine Tools and Manufacture,* vol. 43, pp. 51-60, 2003.

[19] N. Hopkinson, R. Hague, and P. Dickens, *Rapid manufacturing: an industrial revolution for the digital age*: John Wiley & Sons, 2006.